

Theory of fluctuations and localized states in amorphous tetrahedrally bonded solids

J. D. Joannopoulos*

Department of Physics, Massachusetts Institute of Technology, Cambridge, Massachusetts 02139

(Received 6 June 1977)

We present a general solution of a Bethe lattice with arbitrary coordination for a Hamiltonian with an arbitrary number of degrees of freedom per site and an arbitrary number of interaction integrals. This solution is used in conjunction with a realistic tight-binding Hamiltonian to study the effects of rings and bond-angle fluctuations on the p -like region and gap region of the electronic density of states of amorphous tetrahedrally bonded solids. It is shown that even for completely connected networks with no dangling bonds, bond-angle fluctuations create well-defined localized states which lie predominantly at the top of the valence band. These fluctuations also account for the steepening of the valence-band edge with disorder as observed experimentally in photoemission measurements. It is shown that rings do not play a direct role in this effect.

I. INTRODUCTION

There are many important theoretical problems in solid-state physics which remain conceptually formidable owing to a lack of complete periodicity. Surfaces and amorphous solids are two large fields involving problems of this type. This is particularly true in the study of amorphous solids where Bloch's theorem is no longer valid in any dimension and one is thus presented with a severe obstacle in trying to formulate any realistic theory—a realistic theory being one which can be compared readily with experiment.

Recent studies of amorphous tetrahedral semiconductors have largely been concerned with the structural nature of the amorphous phase and with the effects of disorder on the electric and vibrational density of states.¹ The density of states is a useful theoretical tool because it is a simple well-defined function, sensitive to both topology and disorder.

There have been many theoretical methods devised to calculate electronic state densities for noncrystalline materials.¹ One very fruitful approach is the cluster-Bethe-lattice method² (CBLM). Given a Hamiltonian, the CBLM allows an *exact* solution of the state density of an *infinite*, connected network of atoms in terms of the local density of states of each atom at the center of a small cluster of this system. The idea is the following. Consider any connected infinite network of atoms with one atom chosen as a reference point. A small cluster surrounding and including this atom is removed from the system. A Bethe lattice³ is then attached to the dangling surface atoms to simulate the effects of the original infinite system. The Bethe lattice is an infinite aperiodic system of atoms in the same coordination as the original system but with no closed rings of bonds. The reasons for using the Bethe lattice as a boundary condition are simple. Mathematically, it al-

lows, *in principle*, an exact solution of the local Green's function (hence the local density of states) of the central atom. Physically, it maintains the connectivity and coordination number of an infinite system. Moreover the density of states of the Bethe lattice is generally smooth and featureless; consequently any structure found in the local density of states can be associated with the local configuration of the central atom.

The procedure for attaching Bethe lattices to the boundary of a cluster are straightforward. Thus, the most difficult task in the CBLM is solving the Bethe lattice itself. Until recently, Bethe lattices have been solved only for the very simplest of Hamiltonians, that is, simple nearest-neighbor tight-binding Hamiltonians with one²⁻⁴ or two^{5,6} interaction parameters.

In this paper, we present a general method for obtaining the solution of a Bethe lattice with arbitrary coordination for a "tight-binding-like" Hamiltonian with an arbitrary number of degrees of freedom per site and an arbitrary number of interaction integrals. This method is applied to solving the Bethe lattice with a realistic six-parameter tight-binding Hamiltonian for a homopolar tetrahedral solid.⁷ This Bethe lattice is then used in conjunction with the CBLM to study the effects of disorder on the electronic density of states.

There are two regions of the density of states that are of particular interest. These are the regions of the complete filled valence band and the region near the gap. Experimental information about the filled valence-band region can be obtained from ultraviolet⁸ (UPS) and x-ray⁹ (XPS) photoemission measurements. These measurements show the typical changes observed in Fig. 1(a) in going from a crystalline (dashed line) to an amorphous (solid line) spectrum. It is convenient to subdivide and label some specific regions in the valence states. The states at the bottom of the valence band are mostly s -like in

character and are thus labeled S in Fig. 1(a). The uppermost states in the valence band are predominantly p -like (labeled P) and bonding in nature, while the M region contains a "mixture" of s - and p -like states. The tendency of the S and M regions to smear in the amorphous phase is now fairly well understood.¹ It is primarily caused by the presence of five-, seven-, and eight-fold rings of bonds in the amorphous phase. The explanation, however, for the shifting of the P -region peak towards E_v remains unclear and controversial.¹ In this paper, therefore, we shall specifically concentrate on the p -like part of the density of states and examine the effects of rings and bond-angle fluctuations on the P region. Our results will show that it is primarily the bond-angle fluctuations and not the rings that can cause a sharper P -region edge in the amorphous phase.

The region near the valence-conduction band gap has again been studied recently with field-effect measurements.^{10,11} Typical results for amorphous Ge or Si are sketched in Fig. 1(b). There is an indication of localized states lying in the gap near the valence- and conduction-band edges. How do localized states arise? Assuming an intrinsic

sample, there are two possibilities: broken bonds and fluctuations. The effects of the former are easily understood. A broken bond creates states which are half-occupied near the center of the gap. With reconstructions these states can move up or down or split into two groups. Assuming a behavior that is similar to surfaces,¹²⁻¹⁵ one group will remain near midgap while the other group will move down and merge partially with the valence band. The effects of fluctuations, however, are a bit more subtle. Anderson¹⁶ was the first to show that localized states can exist in a solid by studying a simple cubic metal with randomly fluctuating site potentials. With the additional work of Mott, Cohen, and others¹⁷ it is currently generally accepted that disorder fluctuations will give rise to localized states which are found near the band edges of the density of states. These conclusions, however, are only based on very generalized and simple models. When applied to tetrahedral semiconductors, care must be taken. In this work, a realistic and local study of disorder is presented. It is shown that in amorphous tetrahedral homopolar solids localized states can exist without dangling bonds, but that these states should lie *predominantly* near the top of the valence band. A discussion of the type of disorder responsible for this is given.

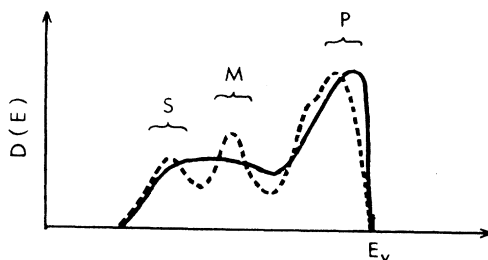
The format of the paper is as follows. In Sec. II we present a general solution to the Bethe lattice. In Sec. III we introduce our Hamiltonian and apply the results of Sec. II to solve the Bethe lattice. Sections IV and V deal with the effects of ring topologies and bond-angle variations, respectively, on the density of states. Finally, in Sec. VI we study how localized states can be created in connected disordered tetrahedral systems.

II. SOLUTION OF BETHE LATTICE

In this section, we present a method that reduces the infinite, coupled equations of the Bethe-lattice Green's-function matrix elements to a finite small set of equations involving the "effective" fields⁵ (or transfer matrices) for this Bethe lattice. Although solutions to this finite set of equations can be obtained in closed form for simple Hamiltonians, more complex Hamiltonians require numerical techniques. These numerical techniques, however, are extremely simple.

We begin by assuming for simplicity that every atom in the Bethe lattice is identical. (The solution can be straightforwardly extended to cases where we have *groups* of atoms that are identical.) We further assume each atom has N nearest neighbors and n degrees of freedom or orbitals. Finally, we assume that the interactions between the

(a) FILLED VALENCE BAND



(b) GAP REGION

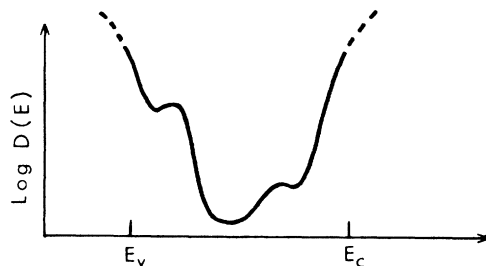


FIG. 1. (a) Sketch of the density of states of a homopolar tetrahedral solid as a function of energy. Amorphous (solid line) and crystalline (dashed line). (b) Sketch of the logarithm of the density of states of an amorphous tetrahedral solid in the gap region as a function of energy.

atoms are confined to nearest neighbors. (This last restriction can be relaxed and treated in a manner discussed at the end of this section.)

In Fig. 2(a) we show schematically a portion of an infinite Bethe lattice for the case $N=3$. There are no closed rings and each dot may be thought of as an n -dimensional vector in the space of degrees of freedom of orbitals for a given atom. (For the case where *groups* of atoms are identical, each dot would represent a group.) Also we adopt the convention that every dot is labeled by a Greek letter α, β, \dots , etc.

Now for the general case of N nearest-neighbor dots the Green's-function matrix-element equations become

$$(E \cdot \mathbf{1}_{\nu\nu} - H_{\nu\nu}) G_{\nu\mu} = \mathbf{1}_{\nu\mu} + \sum_{\lambda}^N H_{\nu\lambda} G_{\lambda\mu}, \quad (1)$$

where E is the energy and H is the Hamiltonian for the electrons. [It is easy to apply (1) to phonons by taking $E \rightarrow M\omega^2$ and $H \rightarrow$ dynamical matrix.] Each "matrix element" in (1) represents an $(n \times n)$ matrix and $\mathbf{1}_{\nu\mu}$ is an $(n \times n)$ unit matrix for $\nu = \mu$ and an $(n \times n)$ zero matrix for $\nu \neq \mu$.

This infinite system of equations (1) can be solved by exploiting two important symmetries of the Bethe-lattice structure: firstly, that every dot can be transformed into any other dot by a fixed set of transformation; secondly, that any two nearest-neighbor dots are connected to each other by only one self-avoiding path. This implies that we can define an "effective" field (or transfer matrix) ϕ_L for each inequivalent line (L) joining any two nearest-neighbor dots that contains all the information concerning the structure away from this line. Thus, in Fig. 2(b) the $N=3$ Bethe lattice is replaced by only one dot interacting with three fields ϕ_A , ϕ_B , and ϕ_C . The Green's function $G_{\mu\mu}$ for this site should be identically equal to the one with the entire Bethe lattice, by defini-

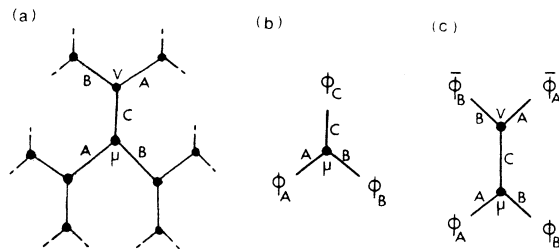


FIG. 2. (a) Portion of a Bethe lattice for a threefold coordinated system. Each dot represents an atom (or a vector of orbitals per site). Only nearest-neighbor interactions are considered. (b) The Bethe lattice represented by a single atom and three "effective" fields. (c) The Bethe lattice represented by two atoms and four "effective" fields.

tion. Thus, we can write immediately for general N ,

$$G_{\mu\mu} = (E \cdot \mathbf{1}_{\mu\mu} - H_{\mu\mu} - M)^{-1}, \quad (2)$$

with

$$M = \sum_{\lambda}^N H_{\mu\lambda} \phi_{L(\lambda)}, \quad (3)$$

where $L(\lambda) = A, B, C, \dots$, etc.

Now this $G_{\mu\mu}$ should be identically equal to the one obtained by just taking two dots and replacing the rest of the system by the corresponding fields. In Fig. 2(c) this is shown for $N=3$ again. The fields $\bar{\phi}_A$ and $\bar{\phi}_B$ are not always equal to ϕ_A and ϕ_B , respectively, because in general

$$(\phi_L, T_L) \neq 0, \quad (4)$$

where T_L transforms ϕ_L to $\bar{\phi}_L$. Thus we now obtain

$$G_{\mu\mu} = [E \cdot \mathbf{1}_{\mu\mu} - H_{\mu\mu} - M + H_{\mu\nu} \phi_{L(\nu)} - H_{\mu\nu} \times (E \cdot \mathbf{1}_{\nu\nu} - H_{\nu\nu} - \bar{M} + H_{\nu\mu}^T \bar{\phi}_{L(\mu)})^{-1} H_{\mu\nu}^T]^{-1}, \quad (5)$$

with

$$\bar{M} = \sum_{\lambda}^N H_{\lambda\nu}^T \bar{\phi}_{L(\lambda)}. \quad (6)$$

If we now compare Eqs. (5) and (2), we obtain

$$\phi_{L(\nu)} = (E \cdot \mathbf{1}_{\nu\nu} - H_{\nu\nu} - \bar{M} + H_{\nu\mu}^T \bar{\phi}_{L(\mu)})^{-1} H_{\mu\nu}^T, \quad (7)$$

and similarly

$$\bar{\phi}_{L(\mu)} = (E \cdot \mathbf{1}_{\mu\mu} - H_{\mu\mu} - M + H_{\mu\nu} \phi_{L(\nu)})^{-1} H_{\mu\nu}. \quad (8)$$

We have now reduced the problem to the solution of the fields ϕ and $\bar{\phi}$ through Eqs. (7) and (8). Once the fields are known $G_{\mu\mu}$ and hence the local density of states $D_{\mu}^i(E)$ for the μ th atom in the i th degree of freedom can be calculated from

$$D_{\mu}^i(E) = -(1/\pi) \text{Im} G_{\mu\mu}^{ii}(E), \quad (9)$$

where $G_{\mu\mu}^{ii}$ is the (i, i) matrix element of the $(n \times n)$ $G_{\mu\mu}$ matrix. In addition, the fields ϕ and $\bar{\phi}$ may be used to attach this Bethe lattice to any finite cluster of atoms.

In many cases Eqs. (7) and (8) can be solved in closed form. In general, however, they are easily solved numerically by iteration.

Let us now return to the case where the interactions between the atoms (or dots) is not confined to nearest neighbors. As an example, we again choose a system with $N=3$. The Bethe lattice including second-nearest-neighbor interactions (as dashed lines) is shown in Fig. 3(a). Note that now the dashed and solid lines form rings of interaction lines. To apply Eqs. (7) and (8) to this system we must transform this structure into a system of groups of atoms interacting in such a way that

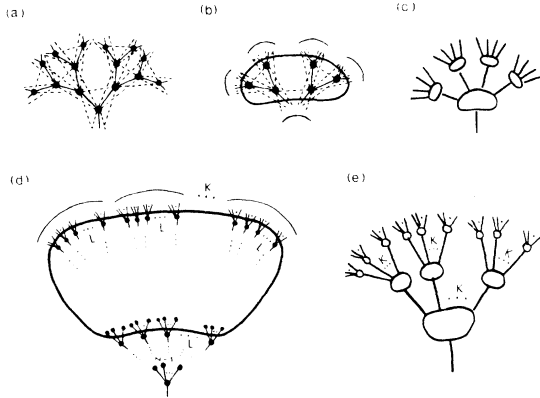


FIG. 3. Transformation of a Bethe lattice of atoms with more than first-neighbor interactions to a Bethe lattice of groups of atoms with only first-neighbor group interactions. (a) Structure of atoms with three first-neighbor interactions (solid lines) and six second-neighbor interactions (dashed lines). Note that the presence of second-neighbor interactions introduces rings of interaction lines and these destroy the Bethe-lattice topology of the original system with only first-neighbor interactions. (b) The structure in (a) may be considered as being made up of groups of atoms as shown here. This group can be represented as a bubble which interacts only with its five nearest-neighbor bubbles. (c) Bethe lattice of bubbles. Each interaction line represents the first- and second-neighbor interactions shown in (a) and (b). (d) Bubble for the general case of N first-neighbor interactions and some arbitrary number of I th-neighbor interactions. For simplicity only the first-neighbor interactions are shown. The bubble is characterized by $L = (N-1)^{(I-2)/2}$ for I even and $L = (N-1)^{(I-3)/2}$ for I odd. (e) Bubbles interact only with $K+1 = (N-1)^I + 1$ other first-neighbor bubbles and form the Bethe lattice shown.

there is only one self-avoiding path between nearest-neighbor groups (i.e., no rings of group-group interactions). This is accomplished by choosing the groups of atoms to be like the one shown in Fig. 3(b). This group interacts with five other groups and can thus be represented in terms of bubbles as shown in Fig. 3(c). This new Bethe lattice may now be solved using the techniques described earlier.

This approach can be generalized to the case of arbitrary N , and an arbitrary number of interaction integrals over a range of I hops. The form the bubble takes is shown in Fig. 3(d). The corresponding Bethe lattice is sketched in Fig. 3(e).

III. APPLICATIONS TO TETRAHEDRALLY BONDED SOLIDS

In order to study the electronic structure of amorphous tetrahedrally bonded solids, we choose a Hamiltonian that is simple enough to be tractable

with nonperiodic structures, yet realistic enough so that it gives a good description of the valence electrons. An excellent candidate for this is the tight-binding Hamiltonian first discussed by Slater and Koster.¹⁸ In this model, one s orbital ($|s\rangle$) and three p orbitals ($|p_x\rangle, |p_y\rangle, |p_z\rangle$) are placed on each site. If only nearest-neighbor atom interactions are included, one obtains six interaction integrals. These may be parametrized and fit to crystalline bulk band structures.^{19,20} The results give (in eV) for Ge

$$\begin{aligned} \langle s|H|s\rangle &\equiv E_s = -6.3, & \langle p|H|p\rangle &\equiv E_p = 2.1, \\ \langle s|H|s'\rangle &\equiv U = -1.7, & \langle p_x|H|p'_x\rangle &\equiv V = 0.7, \\ \langle p_x|H|p'_y\rangle &\equiv T = 1.7, & \langle s|H|p'_x\rangle &\equiv X = 1.4. \end{aligned} \quad (10)$$

A portion of the Bethe lattice for this system is shown in Fig. 4(a). Thus, $N=4$ and each dot represents the $n=4$ orbitals per site which are taken to be a vector (p_x, p_y, p_z, s) . Every tetrahedron is chosen to be in an eclipsed configuration with its nearest neighbors and the four distinct bonds of each atom are labeled $A, B, C,$ and D . Thus, there are eight effective fields for this system which are shown in Fig. 4(b). Equation (2) for the electronic Green's function then becomes

$$G_{00} = (E \cdot \mathbf{1}_{00} - H_{00} - M)^{-1}, \quad (11)$$

where

$$M = H_{01}\phi_A + H_{02}\phi_B + H_{03}\phi_C + H_{04}\phi_D, \quad (12)$$

with

$$H_{00} = \begin{pmatrix} E_p & 0 & 0 & 0 \\ 0 & E_p & 0 & 0 \\ 0 & 0 & E_p & 0 \\ 0 & 0 & 0 & E_s \end{pmatrix} \quad (13)$$

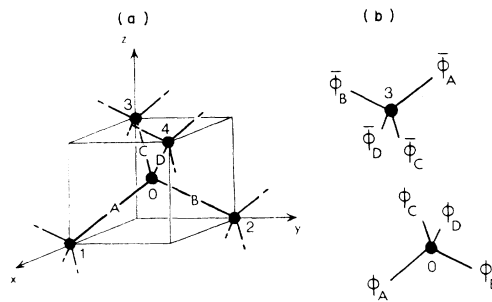


FIG. 4. (a) Portion of a Bethe lattice and choice of coordinate system for a homopolar tetrahedral structure. (b) This Bethe lattice may be presented as either atom 0 or atom 3 with the corresponding effective fields.

and

$$H_{01} = \begin{pmatrix} V & -T & -T & -X \\ -T & V & T & X \\ -T & T & V & X \\ X & -X & -X & U \end{pmatrix}. \quad (14)$$

It is easy to see that the various H_{0n} 's transform into each other by making parity transformations on two axes of the coordinate system. Thus, for example,

$$H_{04} = H_{01} \begin{pmatrix} y \rightarrow -y \\ z \rightarrow -z \end{pmatrix} = H_{02} \begin{pmatrix} x \rightarrow -x \\ z \rightarrow -z \end{pmatrix} = \text{etc.} \quad (15)$$

The fields ϕ_L are the unknown quantities in (11) and can be taken to be of the form

$$\phi_A(E) = \begin{pmatrix} \alpha & -\beta & -\beta & -\gamma \\ -\beta & \alpha & \beta & \gamma \\ -\beta & \beta & \alpha & \gamma \\ -\bar{\gamma} & \bar{\gamma} & \bar{\gamma} & \delta \end{pmatrix}, \quad (16)$$

The various $\phi_{L(n)}$'s transform into each other in a similar way as the corresponding H_{0n} 's. Thus, for example,

$$\phi_D = \phi_A \begin{pmatrix} y \rightarrow -y \\ z \rightarrow -z \end{pmatrix} = \phi_B \begin{pmatrix} x \rightarrow -x \\ z \rightarrow -z \end{pmatrix} = \text{etc.} \quad (17)$$

The unknowns α , β , γ , $\bar{\gamma}$, and δ are obtained by solving (7) with the added symmetry condition

$$\bar{\phi}_L = T_L \phi_L T_L^{-1}, \quad (18)$$

where T_L is diagonal in the parity eigenvalues of the orbitals. Equation (7) is then solved using the numerical technique discussed in Sec. II. Equation (11) then gives

$$\frac{1}{4} T_r G_{00}(E) = \frac{3}{4} G_{00}^{p_x p_x}(E) + \frac{1}{4} G_{00}^{ss}(E), \quad (19)$$

where

$$G_{00}^{p_x p_x}(E) = [E - E_p - 4(\alpha V + 2\beta T + \bar{\gamma} X)]^{-1}, \quad (20)$$

$$G_{00}^{ss}(E) = [E - E_s + 4(3\gamma X - \delta U)]^{-1}. \quad (21)$$

The local densities of states (9) corresponding to the local Green's functions (19)–(21) are shown in Fig. 5. The total density of states for the Bethe lattice is shown at the top of the figure along with a superimposed (dashed line) crystalline diamond spectrum. The filled valence bands lie at negative energies while a portion of the empty conduction bands is shown at positive energies. The two peaks near the bottom of the crystalline valence and conduction bands become smeared out in the Bethe lattice. In addition, the gap becomes larger, but the steep shoulder (near -2 eV) remains essentially unchanged.

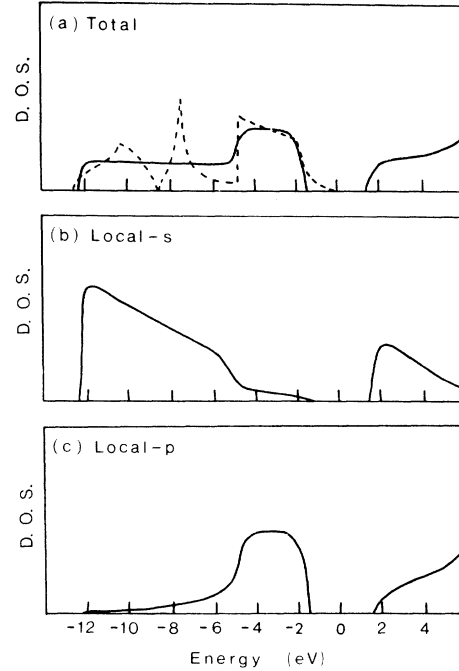


FIG. 5. Densities of states for the Bethe lattice using the Hamiltonian described in the text. The filled valence bands lie at negative energies. (a) Total density of states with superimposed (dashed line) crystalline density of states. (b) Local density of states of the s orbitals. (c) Local density of states of the p orbitals.

The local densities of states for the s orbitals and p orbitals in the Bethe lattice are shown in Figs. 5(b) and 5(c), respectively. As expected, the lower-energy regions of the valence and conduction bands tend to be s -like “bonding” and “antibonding,” respectively, while at larger energies one finds predominantly “bonding” and “antibonding” p -like states, respectively.

All in all, the Bethe-lattice results tend to reproduce most of the features observed in the experimental results in Fig. 1(a). In particular, the smearing of states near the lower part of the density of states is now well understood and attributed to the sensitivity of s -like electrons to topology.¹ What is not reproduced, however, is the pronounced shift of states in the p -like part of the amorphous spectrum towards higher energies which results in a steepening of the shoulder edge. It is the effects of disorder on the p -like region, then, that we wish to concentrate on in the next sections.

IV. RING TOPOLOGIES

In this section, we examine the effects of ring topologies on the local densities of states of atoms situated on rings. For simplicity, we shall concentrate only on sixfold and fivefold rings. A dis-

discussion of the results obtained will be given in Sec. IV C.

A. Sixfold rings

In Fig. 6 we show one sixfold ring in the diamond-structure configuration. To each dangling bond we attach a Bethe lattice. We wish to calculate the local density of states of atom 0. Equation (1) for the system then becomes

$$\begin{aligned} G_{00} &= \Delta^{-1} + H_A G_{10} + H_B G_{50} + A_{CD} G_{00}, \\ G_{10} &= \bar{H}_A G_{00} + \bar{H}_C G_{20} + \bar{A}_{BD} G_{10}, \\ G_{20} &= H_C G_{10} + H_B G_{30} + A_{AD} G_{20}, \\ G_{30} &= \bar{H}_B G_{20} + \bar{H}_A G_{40} + \bar{A}_{CD} G_{30}, \\ G_{40} &= H_A G_{30} + H_C G_{50} + A_{BD} G_{40}, \\ G_{50} &= \bar{H}_B G_{00} + \bar{H}_C G_{40} + \bar{A}_{AD} G_{50}, \end{aligned} \quad (22)$$

where

$$\Delta = E \cdot 1_{00} - H_{00}, \quad (23)$$

$$H_A \equiv \Delta^{-1}(H_{01}) = \Delta^{-1}(H_{43}),$$

$$\bar{H}_A \equiv \Delta^{-1}(H_{01}^T) = \Delta^{-1}(H_{43}^T), \quad (24)$$

$$\begin{array}{c} \cdot \\ \cdot \\ \cdot \end{array}$$

$$\bar{H}_C \equiv \Delta^{-1}(H_{21}^T) = \Delta^{-1}(H_{45}^T),$$

and

$$A_{LM} = H_L \phi_L + H_M \phi_M, \quad (25)$$

$$\bar{A}_{LM} = \bar{H}_L \bar{\phi}_L + \bar{H}_M \bar{\phi}_M.$$

After some algebra, Eq. (22) gives

$$G_{00} = (1_{00} - H_A N_A - H_B N_B - A_{CD})^{-1} \Delta^{-1}, \quad (26)$$

where

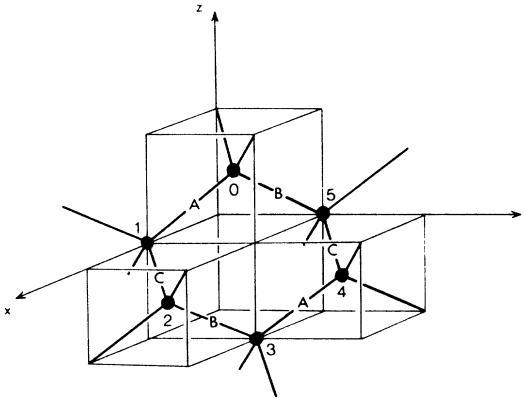


FIG. 6. Sixfold ring in the diamond-structure configuration. Bethe lattices are attached to the dangling bonds.

$$\begin{aligned} N_A &= \Theta_{AB} \bar{\Sigma}_{BD} (\bar{H}_A + \bar{H}_C \Gamma_{BA} \Sigma_{AD} H_B \Psi_{BA} \\ &\quad \times \bar{\Sigma}_{CD} \bar{H}_A \Lambda_{AB} \Sigma_{BD} H_C \bar{\Sigma}_{AD} \bar{H}_B), \end{aligned} \quad (27)$$

$$\begin{aligned} N_B &= \Theta_{BA} \bar{\Sigma}_{AD} (\bar{H}_B + \bar{H}_C \Gamma_{AB} \Sigma_{BD} H_A \Psi_{AB} \\ &\quad \times \bar{\Sigma}_{CD} \bar{H}_B \Lambda_{BA} \Sigma_{AD} H_C \bar{\Sigma}_{BD} \bar{H}_A), \end{aligned} \quad (28)$$

and

$$\begin{aligned} \Sigma_{LM} &= (1_{00} - A_{LM})^{-1}, \\ \bar{\Sigma}_{LM} &= (1_{00} - \bar{A}_{LM})^{-1}, \\ \Lambda_{AB} &= (1_{00} - \Sigma_{BD} H_C \bar{\Sigma}_{AD} \bar{H}_C)^{-1}, \\ \Lambda_{BA} &= (1_{00} - \Sigma_{AD} H_C \bar{\Sigma}_{BD} \bar{H}_C)^{-1}, \\ \Psi_{BA} &= (1_{00} - \bar{\Sigma}_{CD} \bar{H}_A \Lambda_{AB} \Sigma_{BD} H_A)^{-1}, \\ \Gamma_{BA} &= (1_{00} - \Sigma_{AD} H_B \Psi_{BA} \bar{\Sigma}_{CD} \bar{H}_B)^{-1}, \\ \Theta_{AB} &= (1_{00} - \bar{\Sigma}_{BD} \bar{H}_C \Gamma_{BA} \Sigma_{AD} H_C)^{-1}. \end{aligned} \quad (29)$$

It is easy to see that result (26) can be extended, simply, to the case where there is another similar sixfold ring attached to bonds C and D of atom 0. Thus, atom 0 is at the intersection of two sixfold rings and one can immediately write

$$G_{00} = (1_{00} - H_A N_A - H_B N_B - H_C N_C - H_D N_D)^{-1} \Delta^{-1}, \quad (30)$$

where N_C and N_D are obtained from (27) and (28) by letting $A \rightarrow C$, $B \rightarrow D$, $C \rightarrow A$, and $D \rightarrow B$. The advantage of using (30) is that the effects of the rings become a bit more pronounced.

B. Fivefold rings

In Fig. 7 we show one fivefold ring in a flat configuration. It is very easy for a tetrahedral system to form a ring like this because there is only about a 1° difference between the ideal tetrahedral bond angle and the fivefold-ring bond angle. Each atom in the ring is taken to have a similar coordinate system as atom 0 in Fig. 6. Thus, the \hat{z} directions for each atom lie in the plane of the ring and are directed radially outward, whereas the \hat{x} and \hat{y} directions lie 45° out of the plane and their projections are shown in the figure as dashed lines. Each atom in the ring is also bonded to two Bethe lattices through bonds C and D which are not shown.

With this choice of coordinate systems every bond in the ring is identical and labeled A . The Green's-function equations then become

$$\begin{aligned} G_{00} &= \Delta^{-1} + H G_{10} + \bar{H} G_{40} + A_{CD} G_{00}, \\ G_{10} &= H G_{20} + \bar{H} G_{00} + A_{CD} G_{10}, \\ G_{20} &= H G_{30} + \bar{H} G_{10} + A_{CD} G_{20}, \\ G_{30} &= H G_{40} + \bar{H} G_{20} + A_{CD} G_{30}, \\ G_{40} &= H G_{10} + \bar{H} G_{30} + A_{CD} G_{40}, \end{aligned} \quad (31)$$

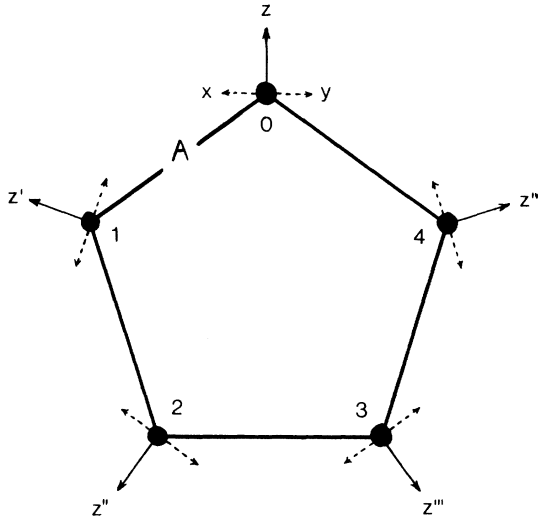


FIG. 7. Flat fivefold ring. The z direction of the coordinate system is chosen to lie in the plane of the ring. The dashed arrows represent the projections of the x and y components onto the plane of the ring. The primed coordinate systems are rotated as discussed in the text.

where

$$H = H_A S, \quad \bar{H} = \Delta^{-1} (\Delta H_A S)^T, \quad (32)$$

and

$$S = \begin{bmatrix} \frac{1}{2}(1 + \cos \frac{2}{5}\pi) & \frac{1}{2}(1 - \cos \frac{2}{5}\pi) & (1/\sqrt{2}) \sin \frac{2}{5}\pi & 0 \\ \frac{1}{2}(1 - \cos \frac{2}{5}\pi) & \frac{1}{2}(1 + \cos \frac{2}{5}\pi) & -(1/\sqrt{2}) \sin \frac{2}{5}\pi & 0 \\ -(1/\sqrt{2}) \sin \frac{2}{5}\pi & (1/\sqrt{2}) \sin \frac{2}{5}\pi & \cos \frac{2}{5}\pi & 0 \\ 0 & 0 & 0 & 1 \end{bmatrix}. \quad (33)$$

S rotates the coordinate system of one atom into the coordinate system of its nearest neighbor. Equations (31) can be solved for G_{00} and give

$$G_{00} = (1_{00} - HN - \bar{H}\bar{N} - A_{CD})^{-1} \Delta^{-1}, \quad (34)$$

where

$$N = \Gamma(\bar{B} + B\bar{\Psi}B\Lambda BB), \quad (35)$$

$$\bar{N} = \bar{\Gamma}(B + \bar{B}\bar{\Psi}\bar{B}\bar{\Lambda}\bar{B}\bar{B}),$$

and

$$B = \Sigma_{CD} H, \quad \bar{B} = \Sigma_{CD} \bar{H},$$

$$\Lambda = (1_{00} - B\bar{B})^{-1}, \quad \bar{\Lambda} = (1_{00} - \bar{B}B)^{-1}, \quad (36)$$

$$\Psi = (1_{00} - B\bar{\Lambda}\bar{B})^{-1}, \quad \bar{\Psi} = (1_{00} - \bar{B}\bar{\Lambda}B)^{-1},$$

$$\Gamma = (1_{00} - B\Psi\bar{B})^{-1}, \quad \bar{\Gamma} = (1_{00} - \bar{B}\bar{\Psi}B)^{-1}.$$

Again, as for the sixfold ring, it is easy to extend result (34) to the case where atom 0 is bonded to two flat fivefold rings lying perpendicular to each

other. The result is

$$G_{00} = [1_{00} - (HN + \bar{H}\bar{N}) - (H'N' + \bar{H}'\bar{N}')]^{-1} \Delta^{-1}, \quad (37)$$

where

$$(H'N' + \bar{H}'\bar{N}') = (HN + \bar{H}\bar{N}) \begin{pmatrix} y \rightarrow -y \\ z \rightarrow -z \end{pmatrix}. \quad (38)$$

C. Results

The local p -like densities of states of an atom at the intersection of two sixfold and two fivefold rings (with Bethe lattices attached outside) are shown in Figs. 8(a) and 8(b), respectively. These are obtained by taking the trace over the p orbitals in Eqs. (30) and (37), respectively. The shape of the bonding p -like region in Fig. 8(a) is rather reminiscent of the shape of the corresponding region in the crystalline spectrum 5(a). This is understandable since the crystal is composed of sixfold rings of exactly the same type as in Fig. 6. Moreover, it is interesting that only a small number of rings are needed to reproduce this shape.

On the other hand, the spectrum in Fig. 8(b) tends to have states concentrated near the center of the bonding p -like bump. This, however, does not shift states up to the top of the band and consequently does not reproduce the steepening of the amorphous spectrum edge. One obtains similar results even with puckered fivefold rings. These can be made as in Fig. 6 by removing atom 3 and connecting atoms 2 and 4 directly. (This also suggests therefore that the effects of dihedral angles are not very important.) Since the shape of a den-

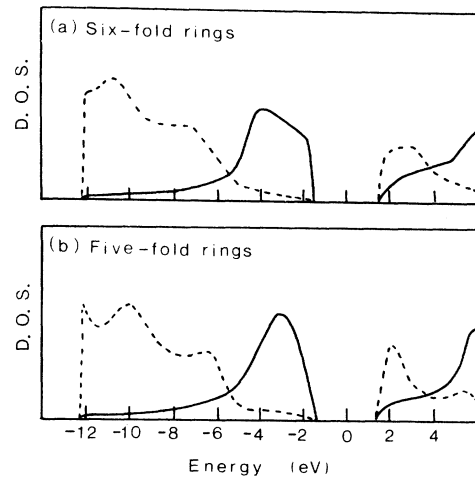


FIG. 8. Local densities of states for an atom at the intersection of two rings with Bethe lattices attached outside. (a) Trace over p -like states (solid line) and s -like states (dashed line) for sixfold rings. (b) Trace over p -like states (solid line) and s -like states (dashed line) for fivefold rings.

sity-of-states spectrum depends mostly on the smallest rings present, it seems reasonable to suggest that higher-order rings would not be able to account for the experimental observations either.

Finally, for completeness, the local s -like densities of states are also shown in Fig. 8 (as dashed lines). As expected, the sixfold-ring versus fivefold-ring character of the spectra are clearly visible.¹

V. BOND-ANGLE VARIATIONS

In this section, we examine variations of bond angles from the ideal tetrahedral value and their effects on the density of states. The procedure is to pick an atom with a disordered configuration of bonds as a reference atom and attach an ideal Bethe lattice to each dangling bond. Since there are no rings of bonds, the local density of states

of the reference atom contains information purely about the effects of bond-angle disorder.

We take the reference atom to be at the origin of our coordinate system. The four unit vectors corresponding to the four bond directions of the disordered tetrahedron are given by

$$n_i = (n_x^i, n_y^i, n_z^i), \quad i = 1, 2, 3, 4. \quad (39)$$

To attach a Bethe lattice to a given bond of the reference atom, we first rotate the coordinate system so that the bond lies along the (111) direction, attach a Bethe lattice with interaction H_D and field ϕ_D [as in Fig. 4(a)] and then, rotate back to the original position. Thus the local Green's function G_{00} of the reference atom is given by

$$G_{00} = \left(\Delta - \sum_i^4 (U_i^{-1} V_i) H_D \phi_D (U_i^{-1} V_i)^T \right)^{-1}, \quad (40)$$

where

$$U_i = \begin{pmatrix} 1 & 1 & 1 \\ \sqrt{3} n_x^i & \sqrt{3} n_y^i & \sqrt{3} n_z^i \\ (n_z^i - n_y^i)/|\sin\theta_i| & (n_x^i - n_z^i)/|\sin\theta_i| & (n_y^i - n_x^i)/|\sin\theta_i| \end{pmatrix}, \quad (41)$$

$$V_i = \begin{pmatrix} (1/\sqrt{3})(2n_y^i + 2n_z^i - n_x^i) & (1/\sqrt{3})(2n_x^i + 2n_z^i - n_y^i) & (1/\sqrt{3})(2n_x^i + 2n_y^i - n_z^i) \\ 1 & 1 & 1 \\ (n_z^i - n_y^i)/|\sin\theta_i| & (n_x^i - n_z^i)/|\sin\theta_i| & (n_y^i - n_x^i)/|\sin\theta_i| \end{pmatrix}, \quad (42)$$

with

$$\cos\theta_i = 1/\sqrt{3} (n_x^i + n_y^i + n_z^i). \quad (43)$$

Since H_D and ϕ_D are known, G_{00} may be calculated for any disordered tetrahedron.

There are two well-known structural models for amorphous tetrahedrally coordinated solids. These are the Polk-Boudreaux²¹ and Connell-Temkin²² random-network models. There is also a crystal-line high-pressure form (ST-12)¹ which contains atoms in disordered tetrahedral arrangements. In Fig. 9, we show the trace of G_{00} over the p orbitals for atoms at the center of the Polk-Boudreaux and Connell-Temkin models, and for an atom of type II in the ST-12 structure. Superimposed (as dashed lines) are the ideal Bethe-lattice results. (The s -like densities of states are not shown because they give spectra which are virtually identical to those of the Bethe lattice.) It is clear, that for all cases, there is a net shift of states to higher energies and a corresponding steepening of the valence-band edge. This is particularly true for the ST-12 spectrum in Fig. 9(c). The large shift of states to the top of the valence-band edge is precisely what is observed for ST-12 using pseudopotentials.¹ It may

now clearly be understood in terms of bond-angle variations.

To get more insight into the effects of bond-angle fluctuations, it is useful to have a way of treating any disordered tetrahedron. To do this we "expand" a disordered tetrahedron into normal mode-like configurations. Since the bond lengths b are held fixed, one can envision a disordered tetrahedron with the interior atom at the center of a sphere of radius b and its four nearest neighbors constrained to lie somewhere on the surface of the sphere. Out of the nine normal modes for a tetrahedron, only five can be generated to satisfy these constraints. These modes would be composed of two configurations of symmetry E and three of symmetry F_2 . Using Fig. 4(a) a typical E configuration would correspond to a clockwise twisting about the \hat{z} axis of bonds A and B and a counterclockwise twisting of bonds C and D . A typical F_2 configuration would have the A - B bond-angle decrease and the C - D bond-angle increase.

The distortions from a perfect tetrahedron can now be written in terms of these five configurations. Indeed, if the distortions are small, one may even write

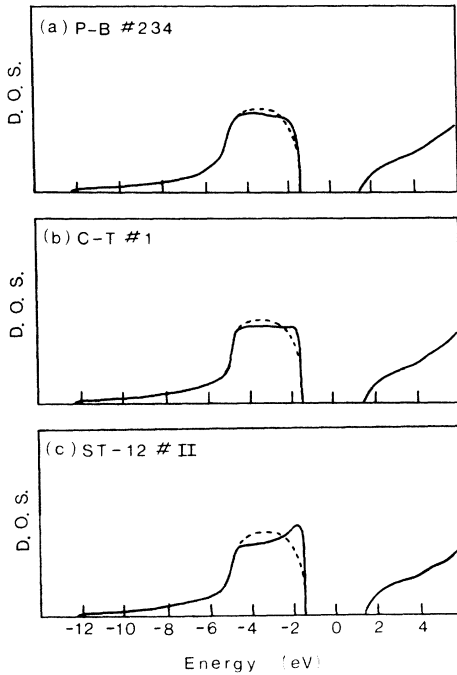


FIG. 9. Trace of p -like densities of states for an atom at the center of a distorted tetrahedral unit with Bethe lattices attached outside. (a) Atom in the configuration of atom No. 234 in the Polk-Boudreaux random-network model. (b) Atom in the configuration of atom No. 1 in the Connell-Temkin random-network model. (c) Atom in the configuration of atom type II in the ST-12 structure. The dashed lines represent the results of an atom in an undistorted tetrahedron (i.e., Bethe lattice).

$$D_0(E, \vec{r}) = D_0(E, 0) + \sum_{i=1}^5 r_i \sum_{n=1}^5 C_{in}^{-1} [D_0(E, \vec{C}_n) - D_0(E, 0)], \quad (44)$$

where $D_0(E, r)$ is the local density of states for the central atom 0 when the four nearest neighbors are at generalized coordinate positions $\vec{r} = \{r_1, r_2, \dots, r_5\}$ with respect to the ideal tetrahedron. The vector $\vec{C}_n = \{C_{1n}, C_{2n}, \dots, C_{5n}\}$ represents the components of a normal-mode configuration n along the generalized coordinate axes. Thus, $D_0(E, \vec{C}_n)$ represents the local state density of atom 0 for a tetrahedron in the n th normal-mode configuration. Since $D_0(E, \vec{C}_n)$ is identical for any mode of the same symmetry, there are only two distinct state density functions. These are shown in Fig. 10 for the F_2 and E configurations. The F_2 spectrum corresponds to $\pm 20^\circ$ changes in two bond angles. The E spectrum is for a configuration with a net twist of 20° . Although the precise shape of $D_0(E, C_n)$ depends on the amount of the distortion in a given normal-mode configuration we are only interested

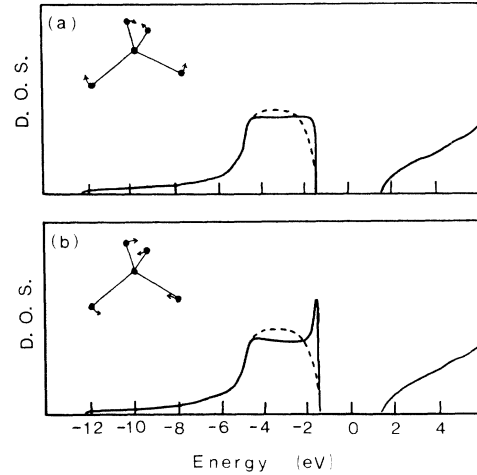


FIG. 10. Trace of p -like densities of states for an atom at the center of a distorted tetrahedral unit with Bethe lattices attached outside. (a) Configuration of symmetry F_2 . Angles changed by $\pm 20^\circ$. Bethe-lattice results shown as dashed lines. (b) Configuration of symmetry E . Twist of 20° . Bethe-lattice results shown as dashed lines.

in observing trends. We note that both give similar results with a steepening of the p -like band edge.

This fact along with (44) suggests that any small bond angle distortions from the ideal tetrahedron will steepen the p -like band edge. This can be understood in terms of a weakening of the p - p' bonding interaction and a shift of occupied p -like states to lower binding energies. In fact, if the distortions were large enough, one might even expect some states to pop out of the valence band into the gap. Indeed, this is what occurs and is the subject of Sec. VI.

VI. LOCALIZED STATES

Since the work of Anderson,¹⁶ it has been known that fluctuations in disordered solids can give rise to localized states which would generally lie near the band edges. The character and precise location of these states, however, would depend on the nature of the fluctuations.

In amorphous tetrahedrally bonded solids, it is known experimentally¹⁷ that the atoms retain their fourfold coordination, apart from some small number of broken bonds. Moreover, the bond lengths in the amorphous phase are virtually unchanged from their crystalline values. The largest fluctuations then in a completed connected structure would arise from bond-angle variations which are typically around ± 10 to $\pm 20^\circ$.

In Sec. V the effects of these fluctuations were studied explicitly in a nonstatistical fashion for

infinite completely connected networks. The states at the top of the valence bands in Figs. 9 and 10 are localized near the disordered site for each system. They are more "resonant-like" in nature, however, since they are degenerate with the bulk Bethe-lattice density-of-states spectrum. Nevertheless bond-angle distortions can create "bonafide" localized states which exist in the gap, even for a completely connected network of atoms. This depends on the nature and amount of the distortion from a perfect tetrahedron. In fact, it is the amount of E character in the distortion that is of crucial importance.

The E configuration tends to flatten out the distorted tetrahedron and make it more "two dimensional." The set of basis orbitals on the central atom, however, is explicitly three dimensional. Consequently, the bonding interaction of one p orbital can be severely reduced in such a structure. As an extreme example, consider the case of an E configuration where the central atom and its four nearest neighbors form a structure that is completely flat. For simplicity, we also take the bond angles in the plane to be 90° . The local density of states of the central atom with non-distorted Bethe lattices attached outside is shown in Fig. 11(a). It is clear that the bonding part of the p orbital perpendicular to the plane has moved out of the valence band and merged with its antibonding part at an energy near the free-atom p -orbital energy $E_p = 2.1$ eV. With a more moderate distortion it would be possible to have the bonding part of this orbital lie in the gap. This is precisely what happens for an atom with the same distortion as *type I* atoms in the ST-12 structure. The local state density is shown in Fig. 11(b). *Type I* atoms exist naturally in a configuration which is mostly of type E . The figure shows one localized state which pops out of the filled valence band. In the crystal, of course, these states would not exist in the gap, but would form bands which would make up the top of the crystalline valence band.

Thus, even for a completely connected system with no bond-length variations, certain types of bond-angle distortions can create localized states which will be found near or in the gap. What is interesting is that our model suggests that these states will only exist near the *top* of the valence band.

Since the ST-12 structure exists in nature it

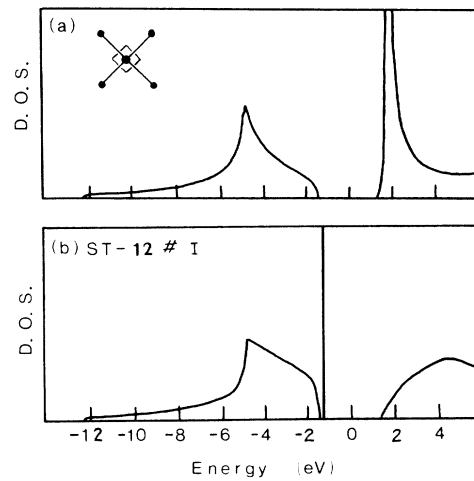


FIG. 11. Trace of p -like densities of states for an atom at the center of a distorted tetrahedral unit with Bethe lattices attached outside. (a) Flat 90° bond-angle configuration. The bonding and antibonding states corresponding to the perpendicular p orbital coalesce near 2.0 eV. (b) Configuration of atom type I in the ST-12 structure. A bona fide localized state produced by bond-angle distortions is represented by a δ function in the density of states.

seems reasonable to assume that distortions similar to and larger than those of type I atoms can also be found in the amorphous phase. These various distorted atoms would then create a region of localized states lying in the gap primarily near the top of the valence band. The bottom of the conduction band and valence band are both s -like in nature and are influenced primarily by the fluctuations in second-nearest-neighbor interactions caused by the bond-angle distortions. These interactions have been neglected in this study because the localized nature of the electrons make the effect of these second-neighbor fluctuations less important.

The experimental situation is yet unclear and it is rather difficult to say what is going on precisely in Fig. 1(b). Nevertheless, mobility measurements on hydrogenated amorphous¹⁰ Si (which should have a negligible number of dangling bonds) show a very low hole mobility. This would seem to be consistent with the predictions of our model for local trapping centers lying primarily at the top of the valence band.

*Supported in part by the Alfred P. Sloan Foundation.

¹For a recent review of electronic properties, see J. D. Joannopoulos and M. L. Cohen, *Solid State Phys.* **31**, 71 (1976); for an excellent study of vibrational

properties, see R. Alben, D. Weaire, J. E. Smith, Jr., and M. H. Brodsky, *Phys. Rev. B* **11**, 2271 (1975).

²J. D. Joannopoulos and F. Yndurain, *Phys. Rev. B* **10**, 5164 (1974).

- ³C. Domb, *Adv. Phys.* 9, 145 (1960).
- ⁴M. Thorpe, D. Weaire, and R. Alben, *Phys. Rev. B* 7, 3777 (1973).
- ⁵J. F. Nagle, J. C. Bonner, and M. F. Thorpe, *Phys. Rev. B* 5, 2233 (1972).
- ⁶F. Yndurain and J. D. Joannopoulos, *Phys. Rev. B* 14, 2569 (1976).
- ⁷A similar solution using different methods has been obtained by V. T. Rajan and F. Yndurain, *Solid State Commun.* 20, 309 (1976).
- ⁸T. M. Donovan and W. E. Spicer, *Phys. Rev. Lett.* 21, 1572 (1968).
- ⁹L. Ley, S. Kowalczyk, R. Pollak, and D. A. Shirley, *Phys. Rev. Lett.* 29, 1088 (1972).
- ¹⁰W. E. Spear and P. G. Le Comber, *Philos. Mag.* 33, 935 (1976), and references therein.
- ¹¹N. F. Mott and E. A. Davis, *Electronic Processes in Non-Crystalline Materials* (Clarendon, Oxford, 1971).
- ¹²J. E. Rowe and H. Ibach, *Phys. Rev. Lett.* 31, 102 (1973).
- ¹³J. E. Rowe, M. M. Traum, and N. V. Smith, *Phys. Rev. Lett.* 33, 1333 (1974).
- ¹⁴A. Coma and R. Ludeke, *Surf. Sci.* 55, 735 (1976).
- ¹⁵P. Chiaradia and S. Nannarone, *Surf. Sci.* 54, 547 (1976).
- ¹⁶P. W. Anderson, *Phys. Rev.* 109, 1492 (1958).
- ¹⁷For references to the various works see Ref. 11.
- ¹⁸J. C. Slater and G. F. Koster, *Phys. Rev.* 94, 1498 (1954).
- ¹⁹J. D. Joannopoulos and M. L. Cohen, *Phys. Rev.* 10, 5075 (1974).
- ²⁰D. J. Chadi and M. L. Cohen, *Phys. Status Solidi B* 62, 235 (1974).
- ²¹D. E. Polk and S. S. Boudreaux, *Phys. Rev. Lett.* 31, 92 (1973).
- ²²G. A. N. Connel and R. J. Temkin, *AIP Conf. Proc.* 20, 192 (1974).